Electrical transport properties in $LiMn_2O_4$, $Li_{0.95}Mn_2O_4$, and $LiMn_{1.95}B_{0.05}O_4$ (B=Al or Ga) around room temperature

E. Iguchi,[a] Y. Tokuda, H. Nakatsugawa, and F. Munakata
Division of Materials Science and Engineering, Graduate School of Engineering, Yokohama National University, Tokiwadai, Hodogaya-Ku, Yokohama, 240-8501 Japan

(Received 24 September 2001; accepted for publication 6 November 2001)

In order to identify the carrier responsible for the electrical transport at room temperature in $LiMn_2O_4$ from the viewpoint of practical applications as a cathode material, the bulk conductivity measurements by complex-plane impedance analyses have been carried out on $LiMn_2O_4$, $Li_{0.95}Mn_2O_4$, and $LiMn_{1.95}B_{0.05}O_4$ ($B=Al^{3+}$ or Ga^{3+}) together with the measurements of four-probe dc conductivities and dielectric relaxation processes, because these are two candidates for the carrier, a Li ion or a nonadiabatic small polaron of an e_g electron on Mn^{3+}. The comparison of the ionic conductivity estimated numerically from the parameters obtained experimentally for the Li-diffusion in $LiMn_2O_4$ with the bulk conductivity indicates that the Li-diffusion seems difficult to play the primary role in the electrical conduction. Instead, a hopping-process of nonadiabatic small polarons of e_g electrons is likely to dominate predominantly the electrical transport properties. The dielectric relaxation process, and the activation energies and the pre-exponential factors of the bulk conductivities in $Li_{0.95}Mn_2O_4$ and $LiMn_{1.95}B_{0.05}O_4$ are explained self-consistently in terms of the polaronic conduction. © *2002 American Institute of Physics.* [DOI: 10.1063/1.1432123]

I. INTRODUCTION

Lithium transition-metal oxides are promising candidates for the cathode materials of rechargeable lithium batteries because of their high voltage and large rechargeable capacities. In particular, the spinel $LiMn_2O_4$ has several advantages such as low cost and low toxicity so that many intensive investigations have been carried out.[1–11]

At ambient temperature, the crystal structure of $LiMn_2O_4$ belongs to the $Fd3m$ space group of a cubic system.[12] The structural phase transformation from $Fd3m$ ($c/a=1$, i.e., cubic) to $I4_1/amd$ ($c/a=1.011$, i.e., tetragonal) occurs at T_t below room temperature.[6,8,13] This transformation is generally attributed to the cooperative Jahn-Teller effect of high spin Mn^{3+} ions. The transformation proceeds with decreasing temperature until the volume fraction of the $I4_1/amd$ phase saturates at 65%. At $T<T_t$, $LiMn_2O_4$ is a small-polaron semiconductor because the e_g electrons on Mn^{3+} ions are trapped in local lattice relaxation sites, and is thermally activated.[6,8,9,14,15]

In our previous experiments on $LiMn_2O_4$,[9] the bulk conductivity obtained by a complex-plane impedance analysis contains the significant knowledge of electrical transport properties. Furthermore the combination of bulk conduction and a dielectric relaxation process, both being obtained in ac measurements, also provides the direct evidence for the electrical transport due to a hopping-process of small polarons below T_t. Electrical properties in $LiMn_2O_4$ at room temperature are most important from the viewpoint of practical applications as a cathode material of rechargeable lithium batteries. In this temperature range, the parameters obtained by impedance analyses and dielectric measurements in our previous study[9] have met mostly the conditions required for a hopping-process of nonadiabatic small polarons.[16,17] However we have hesitated to accept a hopping-process, and a final conclusion is still postponed because there is another strong candidate for the carrier, i.e., Li^+ ions. We should never omit the possibility of the ionic conduction due to the Li-diffusion. In order to identify the carrier in the spinel $LiMn_2O_4$ at $T>T_t$, a nonadiabatic small polaron of an e_g electron or a Li-ion, the experiment of Verhoeven *et al.* on the lithium dynamics probed directly by two-dimensional[7] Li NMR with the result of the activation energy for the Li-diffusion, i.e., 0.5 ± 0.1 eV, in the temperature range of 345–400 K,[18] and the chemical diffusion coefficient of lithium in $LiMn_2O_4$ for the temperature range of 263–333 K obtained by Munakata *et al.*,[19] i.e., $D=2.5\times10^{-5}\times\exp(-0.26/k_BT)$ cm^2/s, are very important.

The main purpose of the present study is to identify the character of the carrier responsible for the electrical transport above T_t. Besides a $LiMn_2O_4$ specimen, two sorts of specimens have been prepared, one is a Li-deficient specimen, i.e., $Li_{1-x}Mn_2O_4$, and another one is $LiMn_{2-x}B_xO_4$ in which Mn^{3+} ions are partially replaced with B^{3+} ($B^{3+}=Al^{3+}$ or Ga^{3+}). These specimens surely promise very useful knowledge as to characters of the carrier because a change in the composition affects the carrier density. The present report will describe the electrical transport phenomena in these materials at room temperature and will discuss the conduction mechanism that dominates the electrical transport properties in $LiMn_2O_4$, which is the most important function of this material for practical applications as a cathode material, referring to the ionic conductivity estimated numerically from the diffusion coefficient of the Li ions in $LiMn_2O_4$.[18,19]

[a]Author to whom correspondence should be addressed; electronic mail: iguchi@post.me.ynu.ac.jp

II. EXPERIMENTAL DETAILS

The specimens of $LiMn_2O_4$, $Li_{0.95}Mn_2O_4$, and $LiMn_{1.95}B_{0.05}O_4$ ($B=Al^{3+}$ or Ga^{3+}) were prepared by the conventional solid-state reaction technique using Li_2CO_3, MnO_2, Al_2O_3 and Ga_2O_3 powders. The mixture was calcined in air at 750 °C for 12 h. After mixing carefully, this heat-treatment was repeated again. After grounding, the calcined powder was pressed into pellets, and finally sintered in air at 850 °C for one day.[1,6,7,20–22] The powder diffraction at room temperature using a Cu $K\alpha$ x-ray indicates a single phase of a cubic spinel structure in every specimen. The lattice constant of $LiMn_2O_4$ at room temperature is 8.2382 Å which agrees with the previous result.[10] When Mn ions are partially replaced with Al^{3+} or Ga^{3+}, the lattice constant increases, i.e., 8.2410 Å for $B=Al^{3+}$ and 8.2448 Å for $B=Ga^{3+}$. Such a difference in the lattice constants is ascribed to the ionic radius of Ga^{3+} bigger than Al^{3+}. As for $Li_{0.95}Mn_2O_4$, the lattice constant is 8.2295 Å which is smaller than $LiMn_2O_4$ mainly because of the Li-deficiency. The grain size of the specimens was found to be $\sim 1\ \mu$m on average by scanning microscope studies. The density of the specimens was about 80% of the theoretical value.

Ac measurements (capacitance and impedance) have been carried out in the same way as our previous reports,[23–27] using the frequency in the range of 100 Hz to 1 MHz. An In–Ga alloy in a 7:3 ratio was used for the electrode. A Maxwell–Wagner-type polarization due to heterogeneity in a specimen is excluded because there are no significant differences in frequency dependencies of dielectric constant at room temperature even if the thickness of the specimen is reduced to 50%. The details of four-probe dc conductivity measurements are described also elsewhere.[23–27]

III. EXPERIMENTAL RESULTS

As described previously,[9,23–27] bulk conductivity and boundary conductivity in a polycrystalline compound are to be obtained independently by the complex-plane impedance analysis based upon the legitimacy which MacDonald[28–30] and Franklin[31] demonstrate. Usually three arcs show in the impedance plots where the imaginary part Z'' of the total impedance is plotted against the real part Z' as a parametric function of frequency, i.e., the highest frequency arc corresponding to the bulk conduction, the intermediate arc due to the conduction across the grain boundary and the lowest frequency arc coming from the transport across the electrode–specimen interface. The resistance values of the circuit elements are obtained by the real part intercepts. Since the electrical transport properties above T_t are to be investigated, dielectric properties at temperatures as high as possible are desired. A Li-electrode would be best towards this end, but the In–Ga alloy is used.[9,23–27] Though the melting point of this alloy is ~ 70 °C, the ac measurements in the temperature range up to 70 °C provide the reliable knowledge of the transport properties in the present system. The trial to use Au or Ag as an electrode has failed.

Figure 1 depicts complex-plane impedance plots at 260 K, 290 K, and 320 K for $LiMn_{1.95}Ga_{0.05}O_4$. Though the highest frequency arc appears at 260 K, the plots of this arc at 290 K and 320 K require frequencies much higher than 1 MHz. However, the lowest resistance values of the intermediate frequency arcs correspond to the bulk resistances. Four-probe dc conductivities were measured up to 400 K mainly so as to confirm that a Li-deficit or any structural change does not arise unexpectedly in heating processes.

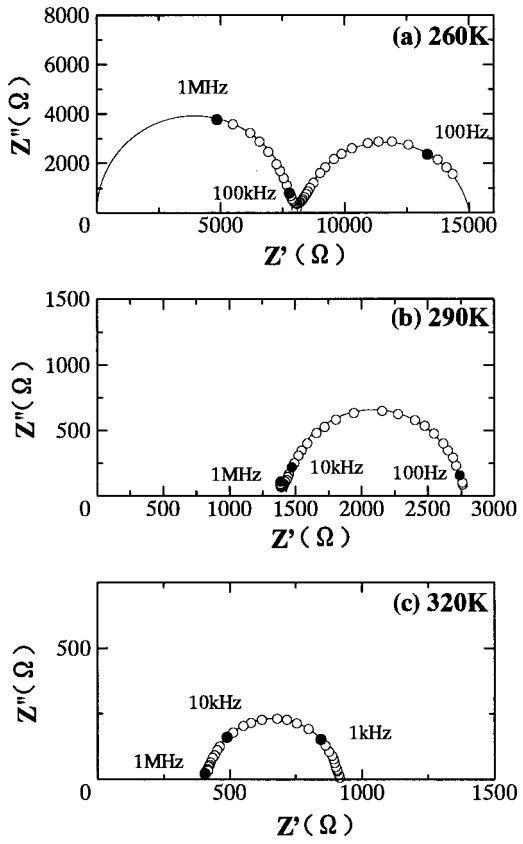

FIG. 1. The complex-plane impedance analyses at 260 K (a), 290 K (b), and 320 K (c) for $LiMn_{1.95}Ga_{0.05}O_4$.

The reproducibility as to $LiMn_2O_4$ prepared here has been checked with reference to the previous experiments on this material.[9] The bulk conductivities measured by the impedance analyses follow an Arrhenius relation: $\log(\sigma T)$ vs $1/T$ with the activation energy of 0.42 eV and the pre-exponential factor of $9.0\times 10^5\ \Omega^{-1}\,\mathrm{cm}^{-1}\,\mathrm{K}$ above room temperature. These parameters agree, within the experimental errors, with the data reported previously,[9] 0.41 eV and $8.5\times 10^5\ \Omega^{-1}\,\mathrm{cm}^{-1}\,\mathrm{K}$. Since $Li_{1-x}Mn_2O_4$ at $x \geqslant 0.1$ is found to involve Mn_3O_4 in the XRD pattern, the specimen of $x=0.5$., i.e., $Li_{0.95}Mn_2O_4$, has been prepared.

Figure 2 illustrates three Arrhenius relations of $\log(\sigma T)$ vs $1/T$ for $LiMn_{1.95}Al_{0.05}O_4$ above T_t, employing the four-probe dc conductivity, the bulk conductivity and the total conductivity in bulks and boundaries. The inset in Fig. 2 depicts the Arrhenius plots of $\log(\sigma T^{3/2})$ vs $1/T$ for the bulk conduction, because the conductivity due to the ionic conduction or the hopping conduction of adiabatic small polarons is represented by $\sigma = A_0 \exp(-Q/k_BT)/T$, whereas the hopping conductivity of nonadiabatic small plarons has a form of $\sigma = A_0' \exp(-Q'/k_BT)/T^{3/2}$, where k_B is the Boltz-

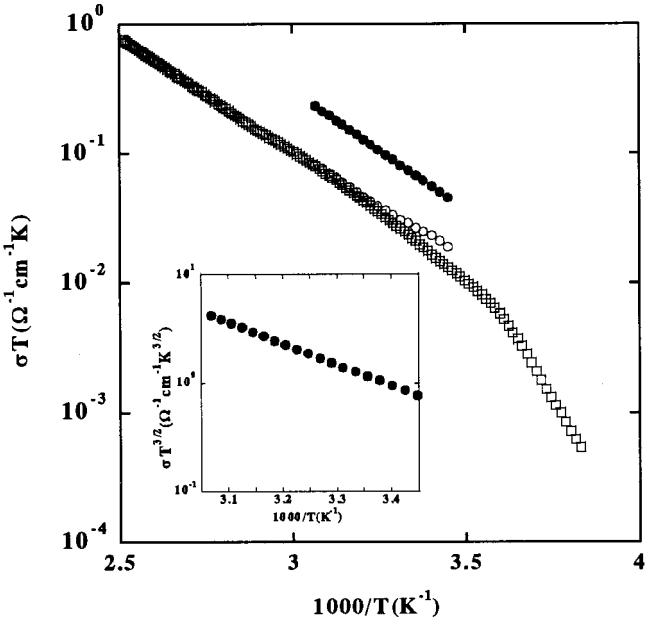

FIG. 2. Three Arrhenius relations of $\log(\sigma T)$ vs $1/T$ for $LiMn_{1.95}Al_{0.05}O_4$; solid circles, open circles, and open squares represent bulk conductivities, total conductivities in bulks and boundaries and four-probe dc conductivities. (Inset) The Arrhenius relation of $\log(\sigma T^{3/2})$ vs $1/T$ for bulk conductivities in $LiMn_{1.95}Al_{0.05}O_4$.

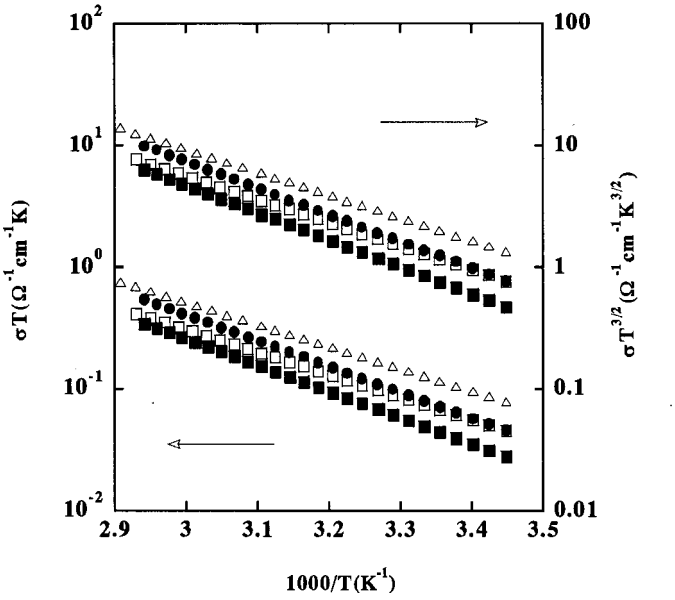

FIG. 3. The Arrhenius relations of $\log(\sigma T)$ vs $1/T$ and $\log(\sigma T^{3/2})$ vs $1/T$ for $LiMn_2O_4$ (solid circles), $Li_{0.95}Mn_2O_4$ (solid squares), $LiMn_{1.95}Ga_{0.05}O_4$ (open triangles), and $LiMn_{1.95}Al_{0.05}O_4$ (open squares).

mann's constant. The linear relations hold in the both plots. If only the temperature dependence of conductivities is employed, the conduction kinetic is generally difficult to identify because the conductivities subject to the adiabatic Arrhenius relation also satisfy currently the nonadiabatic one. The linear relation in the Arrhenius plots as to four-probe dc conductivity prolonged to 400 K assures that neither the Li-deficit nor any structural change occurs during measurements. The similar relation holds for each specimen. Employing the bulk conductivities, Fig. 3 plots the Arrhenius relations, $\sigma T = A_0 \exp(-Q/k_BT)$ and $\sigma T^{3/2} = A_0' \exp(-Q'/k_BT)$, for every specimen. Table I summarizes the values for Q, A_0, Q', and A_0' for each specimen.

Every specimen shows the dielectric relaxation process just like $LiMn_2O_4$.[9] Figure 4 illustrates the frequency dependencies of dielectric loss tangent ($\tan\delta$) as a parametric function of temperature at 2 K increments in the range of 286–326 K for $LiMn_{1.95}Al_{0.05}O_4$. The resonance behavior in loss tangent changes distinctly at 294 K. This is due to the phase transition, as observed in $LiMn_2O_4$.[9] Despite the similar dielectric behaviors, the details of the relaxation processes in $LiMn_{1.95}Al_{0.05}O_4$ and $LiMn_2O_4$ differ. In fact, the relaxation peak of electric modulus (imaginary part M'') is measurable only below 264 K in $LiMn_{1.95}Al_{0.05}O_4$, but observable in $LiMn_2O_4$ up to 335 K.[9] $LiMn_{1.95}Ga_{0.05}O_4$ exhibits the dielectric behavior similar to $LiMn_{1.95}Al_{0.05}O_4$.

IV. DISCUSSION

A. Numerical estimations of ionic conductivities due to Li-diffusion

Numerical estimations of ionic conductivities based upon the experiments on the Li-diffusion[18,19] are indispensable for the present primary purpose because it must be possible to presume the process dominating the electrical transport by comparing the ionic conductivities with the bulk conductivities. Referring to the theories to diffusion in ionic compounds,[32,33] the Li-diffusion in $LiMn_2O_4$ has a form of $D \cong g\nu a^2 \exp(-E/k_BT)$, where g, ν, a, and E are the geometrical constant, the lattice frequency, the distance over which the Li ions jump, and the energy required for the diffusion. Since the Li ions are expected to migrate in interstitial paths, the assistance of vacancies is unnecessary.

In Einstein's model,[31] the ionic conductivity is represented by $\sigma = Ne^2D/k_BT \cong Ng\nu a^2e^2 \exp(-E/k_BT)/k_BT$, where N is the concentration of the Li ions in $LiMn_2O_4$, i.e., $N \cong 1.4\times10^{22}/cm^3$. Two-dimensional ^{7}NMR measurements yield $E = 0.5 \pm 0.1$ eV and $a = 1.78$ Å.[18] Then $\sigma/g\nu = (2.7\times10^{-8} - 2.5\times10^{-5})$ (dimensionless) at 340 K, where ν is unknown but g is generally less than 1.0. If the ionic conduction due to the Li-diffusion is the main process above T_t, the bulk conductivity $1.6\times10^{-3}\ \Omega^{-1}\,cm^{-1}$ in $LiMn_2O_4$ obtained at 340 K in the present study requires the lattice frequency ν in the range of $5.8\times10^{13}\ s^{-1}$ to $5.3\times10^{16}\ s^{-1}$, where $g \cong 1$. Though the Debye temperature Θ_D and the De-

TABLE I. Activation energies and pre-exponential factors Q (eV), A_0 ($\Omega^{-1}\,cm^{-1}\,K$), Q' (eV), and A_0' ($\Omega^{-1}\,cm^{-1}\,K^{3/2}$) which are involved in conductivities, $\sigma = A_0 \exp(-Q/k_BT)/T$ and $\sigma = A_0' \exp(-Q'/k_BT)/T^{3/2}$, for every specimen.

	Q (eV)	A_0 ($\Omega^{-1}\,cm^{-1}\,K$)	Q' (eV)	A_0' ($\Omega^{-1}\,cm^{-1}\,K^{3/2}$)
$LiMn_2O_4$	0.42	9.0×10^5	0.44	2.6×10^7
$Li_{0.95}Mn_2O_4$	0.42	7.6×10^5	0.44	2.2×10^7
$LiMn_{1.95}Ga_{0.05}O_4$	0.36	1.4×10^5	0.37	4.1×10^6
$LiMn_{1.95}Al_{0.05}O_4$	0.37	1.2×10^5	0.38	3.3×10^6

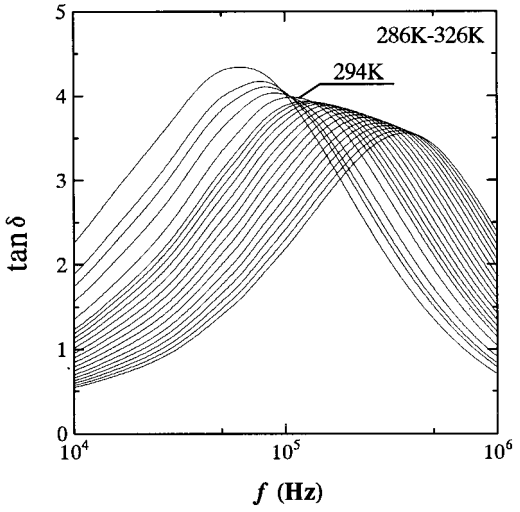

FIG. 4. Frequency dependencies of dielectric loss tangent (tan δ) as a parametric function of temperature at 2 K increments in the temperature range of 286–326 K for $LiMn_{1.95}Al_{0.05}O_4$.

bye frequency ν_m in $LiMn_2O_4$ are unknown, ν_m in most solids is generally less than $\sim 10^{13}$ s^{-1}.[34] If the Debye temperature in Li is used for reference,[34] i.e., $\Theta_D = 344$ K, the relation of $k_B\Theta_D = h\nu_m$ yields $\nu_m = 3\times 10^{12}$ s^{-1}. Since the real lattice frequency is less than ν_m, the ionic conduction due to the Li-diffusion seems difficult to govern the electrical transport at $T > T_t$, although the activation energy required for the Li-diffusion obtained by Verhoeven *et al.*[18] and that of the bulk conduction are in agreement within the experimental errors.

If based upon the result of Munakata *et al.*,[19] the numerical formula of $D = 2.5\times 10^{-5}\exp(-0.26/k_BT)$ cm^2/s yields the ionic conductivity at 340 K, $\sigma = 2.6\times 10^{-4}$ $\Omega^{-1}\,cm^{-1}$, which is about 15% of the bulk conductivity, 1.6×10^{-3} $\Omega^{-1}\,cm^{-1}$. Then the Li-diffusion is difficult to play the primary role in the electrical transport at $T > T_t$. Furthermore, the activation energy required in the Li-diffusion is remarkably different from that in the bulk conduction.

These assessments of the ionic conductivities deduce that the effective contribution of the ionic conduction to the bulk conduction must be small, and instead the non-adiabatic hopping conduction seems predominantly responsible for the electrical transport at $T > T_t$.

B. Reduction of activation energy in $LiMn_{1.95}B_{0.05}O_4$

$LiMn_2O_4$ and $Li_{0.95}Mn_2O_4$ have nearly equal activation energies, implying weak interactions between Li ions in the present system, as Munakata *et al.* indicate.[19] The speculation described above indicates that $Q' = 0.44$ eV in $LiMn_2O_4$ is nearly equal to the hopping energy of nonadiabatic e_g small polanons, i.e., W_H. However, the activation energy reduces to $Q' \cong 0.38$ eV in $LiMn_{1.95}B_{0.05}O_4$. The activation energy required for the polaronic conduction has a form of $Q' \cong W_H = W_P/2 - t$, where W_P is the polaron binding energy and $2t$ is the $3d$-narrow band width.[35]

A polaron is stabilized through a local deformation of the lattice due to the electron–phonon interactions.[34,36–39] The local deformation caused by the drawing together of the ions in the bond via the electron–phonon interactions results in the lattice deformation energy E_D which is positive, and also the electron–phonon interaction energy E_{ep} which is negative. The polaron binding energy is given by $W_P = -(E_D + E_{ep})$. When $|E_{ep}| > E_D$, the polaron is stabilized.[35] Totally the activation energy has a form of $Q' \cong -(E_D + E_{ep})/2 - t$. In $LiMn_{1.95}B_{0.05}O_4$, B-substitution for Mn^{3+} decreases the amount of Mn^{3+} ions. Then the overlapping probability of Mn $3d$ wave functions decreases and the band width never expands, even if it becomes narrow. Consequently the activation energy decreases owing to either an increase in E_D or a decrease in $|E_{ep}|$.

In the $LiMn_2O_4$-system, the e_g electron on Mn^{3+} ion has a Jahn-Teller effect which distorts the lattice field around Mn^{3+} cooperating with the electron–phonon interactions. Al^{3+} and Ga^{3+} have the similar electronic structures but no e_g electrons, i.e., ns^2np^6 ($n=2$ for Al^{3+} and 3 for Ga^{3+}). The spinel structure contains a network of edge sharing MnO_6 octahedra through O^{2-} ions. When Al^{3+} (or Ga^{3+}) is substituted for Mn^{3+} at the center of a MnO_6 octahedron, six $2p$ (or $3p$) electrons on Al^{3+} (or Ga^{3+}) push away the O^{2-} ions shared with the neighboring MnO_6 octahedra because of the repulsive coulombic interactions between p electrons in Al^{3+} (or Ga^{3+}) and O^{2-}. The lattice deformation caused by the displacement of these O^{2-} ions due to Al^{3+} (or Ga^{3+}) in addition to the deformation due to the Jahn-Teller effect and electron–phonon interactions increases the deformation energy E_D. As a result, the polaron binding energy in $LiMn_{1.95}B_{0.05}O_4$ becomes small in comparison with $LiMn_2O_4$ and accordingly the activation energy decreases. Since n in Ga is bigger than Al, the displacement of O^{2-} ions due to Ga^{3+} must be larger than Al^{3+} and the activation energy in $LiMn_{1.95}Ga_{0.05}O_4$ is somewhat smaller than $LiMn_{1.95}Al_{0.05}O_4$.

C. Pre-exponential factors

The pre-exponential factors A_0' for $Li_{0.95}Mn_2O_4$ and $LiMn_{1.95}B_{0.05}O_4$ are smaller than that in $LiMn_2O_4$ as shown in Table I. In the theory to nonadiabatic small polarons,[35,39,40] $A_0' = ne^2a^2\pi^{1/2}J^2/2\hbar k_B^{3/2}W_H^{1/2}$, where n is the density of nonadiabatic small polarons, e denotes the electronic charge, and J is the electron transfer integral between neighboring Mn ions. Then the reduction in W_H must increase A_0' of $LiMn_{1.95}B_{0.05}O_4$. Nevertheless, the pre-exponential factors in these materials become smaller than $LiMn_2O_4$. This implies that the carrier-density n contributes more directly to the reduction in A_0' than W_H.

In $LiMn_{1.95}B_{0.05}O_4$, the electrical neutrality requires a decrease in Mn^{3+} implying a decrease in the density of e_g electrons compared to $LiMn_2O_4$. However, the amount of Li ions does not change upon B-substitution for Mn^{3+}. Then A_0' in $LiMn_{1.95}B_{0.05}O_4$ smaller than $LiMn_2O_4$ suggests that the hopping conduction is predominant at $T > T_t$. In $Li_{0.95}Mn_2O_4$, A_0' is also smaller slightly than $LiMn_2O_4$ but it seems difficult to identify the carrier by the speculation on pre-exponential factors because this oxide contains two pos-

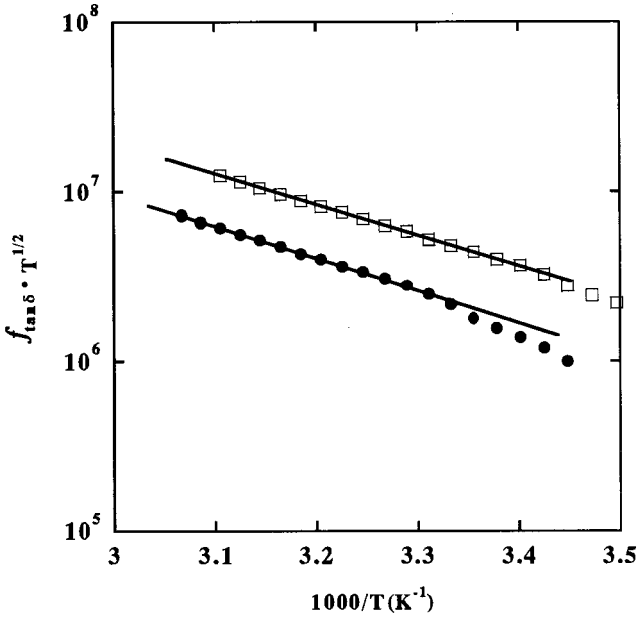

FIG. 5. The Arrhenius relation between $\log(f_{\tan\delta}T^{1/2})$ and $1/T$ for $LiMn_{1.95}Ga_{0.05}O_4$ (open squares) and $LiMn_{1.95}Al_{0.05}O_4$ (solid circles).

sibilities, i.e., the reduction of Li-density or the decrease in the amount of Mn^{3+}.

D. Dielectric relaxation process

In general, polaronic conduction involves a dielectric relaxation process that is described by the Debyes theory,[40,41] and the combination of the resonance frequencies in loss tangent and modulus at a temperature T calculates the activation energy required for the hopping conduction.[9,23,42] $LiMn_{1.95}B_{0.05}O_4$ exhibits the dielectric relaxation in loss tangent as shown in Fig. 4, but the relaxation peaks in electric modulus are not obtainable at $T>T_t$. In such a case, the activation energy is usually tried to obtain employing the approximation of $\tan\delta \propto \epsilon''$.[43–45] Using the resonance frequency $f_{\tan\delta}$ in loss tangent at a temperature T, then, there is the relation of $f_{\tan\delta}T^{1/2} \propto \exp(-Q'/k_BT)$ in the case of nonadiabatic small polarons.[9,43–45]

Figure 5 demonstrates the Arrhenius relations of $\log(f_{\tan\delta}T^{1/2})$ vs $1/T$ for $LiMn_{1.95}B_{0.05}O_4$ with $Q'=0.38$ eV for $B=Al^{3+}$ and 0.36 eV for $B=Ga^{3+}$. The slight deviation from the linear relation at lower temperatures is due to the phase transition. Despite this approximation, the activation energies estimated in this way are nearly equal to those of the bulk conduction. $Li_{0.95}Mn_2O_4$ exhibits the dielectric relaxation behavior very similar to $LiMn_2O_4$.[9] The electrical conduction in the $LiMn_2O_4$-system at room temperature involves then a dielectric relaxation process, which is very advantageous to the polaronic conduction. These ac results suggest certainly that non-adiabatic hopping conduction takes place in the $LiMn_2O_4$-system.

V. CONCLUSION

The electrical transport properties in $LiMn_2O_4$ at room temperature are important from the viewpoint of practical applications as a cathode material of rechargeable lithium batteries. Since there are two candidates for the carrier at room temperature, a Li ion or a nonadiabatic small polaron of e_g electrons on Mn^{3+} ion, the bulk conductivity measurements by complex-plane impedance analyses have been carried out on $LiMn_2O_4$, $Li_{0.95}Mn_2O_4$, and $LiMn_{1.95}B_{0.05}O_4$ ($B=Al^{3+}$ or Ga^{3+}) together with the measurements of four-probe dc conductivities and dielectric relaxation processes. The dc conductivity measured up to 400 K indicates that there are no anomalies due to a Li-deficit and any structural change during measurements. Employing the results on the Li-diffusion in $LiMn_2O_4$, the ionic conductivities have been estimated numerically and compared with the bulk conductivities in this material. This comparison deduces that the ionic conduction due to the Li-diffusion seems difficult to play a primary role in the electrical transport at room temperature. Instead, a hopping-process of nonadiabatic small polarons is likely to be the main process. This deduction is evidenced by the reduction in the activation energies and the pre-exponential factors of the bulk conductivities in $LiMn_{1.95}B_{0.05}O_4$. The dielectric relaxation process in loss tangent observed in every specimen is also in favor of the polaronic conduction in $LiMn_2O_4$ around room temperature.

ACKNOWLEDGMENTS

The authors are very grateful to S. Nakamura for his assistance in this project. This project was supported by Takahashi Industrial and Economic Research Foundation.

[1] M. M. Thackeray, W. I. F. David, P. G. Bruce, and J. B. Goodenough, Mater. Res. Bull. **18**, 461 (1983).
[2] J. M. Tarascon and D. Guyomard, J. Electrochem. Soc. **138**, 2864 (1991).
[3] D. Guyomard and J. M. Tarascon, J. Electrochem. Soc. **139**, 937 (1992).
[4] B. Scrosati, J. Electrochem. Soc. **139**, 2776 (1992).
[5] T. Ohzuki, *Lithium Batteries*, edited by G. Pistoia (Elsevier Science, Amsterdam, 1994), p. 239.
[6] J. Sugiyama, T. Tamura, and H. Yamauchi, J. Phys.: Condens. Matter **7**, 9755 (1995).
[7] J. Sugiyama, T. Atsumi, T. Hioki, S. Noda, N. Kamegashira, and J. Sugiyama, J. Alloys Compd. **235**, 163 (1996).
[8] J. Sugiyama, T. Atsumi, K. Koiwai, T. Sasaki, T. Hioki, S. Noda, and N. Kamegasira, J. Phys.: Condens. Matter **9**, 113 (1997).
[9] E. Iguchi, N. Nakamura, and A. Aoki, Philos. Mag. B **78**, 65 (1998).
[10] J. Molenda, K. Swierczek, W. Kucza, J. Marzec, and A. Stoklosa, Solid State Ionics **123**, 155 (1999).
[11] V. Massarotti, D. Capsoni, M. Bini, G. Chiodelli, C. B. Azzoni, M. C. Mozzati, and A. Paleari, J. Solid State Chem. **131**, 94 (1997).
[12] K. Miura, A. Yamada, and M. Tanaka, Electrochim. Acta **41**, 249 (1996).
[13] A. Yamada and M. Tanaka, Mater. Res. Bull. **30**, 715 (1995).
[14] J. B. Goodenough, A. Manthiram, and B. Wnertzewski, J. Power Sources **43–44**, 269 (1993).
[15] L. Schütte, G. Colsmann, and B. Reuter, J. Solid State Chem. **27**, 227 (1979).
[16] T. Holstein, Ann. Phys. (N.Y.) **8**, 343 (1959).
[17] D. Emin, Phys. Rev. B **4**, 3112 (1971).
[18] V. W. J. Verhoeven, I. M. deSchepper, G. Nachtegaal, A. P. M. Kentgens, E. M. Kelder, J. Schoonman, and F. E. Mulder, Phys. Rev. Lett. **86**, 4314 (2001).
[19] F. Munakata, T. Ito, Y. Ohsawa, and M. Kawai, J. Mater. Sci. Lett. (to be published).
[20] D. G. Wickham and W. J. Croft, J. Phys. Chem. Solids **7**, 351 (1958).
[21] W. I. F. David, M. M. Thackeray, L. A. DePicciotto, and J. B. Goodenough, J. Phys. Chem. Solids **67**, 316 (1987).
[22] A. Yamada, J. Phys. Chem. Solids **122**, 160 (1996).
[23] E. Iguchi, K. Ueda, and W. H. Jung, Phys. Rev. B **54**, 17431 (1996).
[24] E. Iguchi, N. Nakamura, and A. Aoki, J. Phys. Chem. Solids **58**, 755 (1997).

[25] H. Nakatsugawa and E. Iguchi, J. Phys.: Condens. Matter **11**, 1711 (1999).
[26] N. Nakamura and E. Iguchi, J. Solid State Chem. **145**, 58 (1999).
[27] E. Iguchi, H. Satoh, H. Nakatsugawa, and F. Munakata, Physica B **270**, 332 (1999).
[28] J. R. MacDonald, J. Chem. Phys. **61**, 3977 (1974).
[29] J. R. MacDonald, *Superionic Conductors* (Plenum, New York, 1976), p. 1.
[30] J. R. MacDonald, *Impedance Spectroscopy* (Wiley, New York, 1987), p. 1.
[31] A. D. Franklin, J. Am. Ceram. Soc. **58**, 465 (1975).
[32] A. J. Dekker, *Solid State Physics* (Prentice–Hall, New York, 1957), Chap. 7.
[33] R. A. Swalin, *Thermodynamics of Solids* (Wiley, New York, 1970), Chap. 15.
[34] C. Kittel, *Introduction to Solid State Physics*, 4th ed. (Wiley, New York, 1971), Chaps. 6 and 11.
[35] I. G. Austin and N. F. Mott, Adv. Phys. **18**, 41 (1969).
[36] P. W. Anderson, Phys. Rev. Lett. **34**, 953 (1975).
[37] E. Iguchi, T. Yamamoto, and R. J. D. Tilley, J. Phys. Chem. Solids **49**, 205 (1988).
[38] E. Iguchi, A. Tamenori, and N. Kubota, Phys. Rev. B **45**, 697 (1992).
[39] I. G. Lang, and A. Yu. Firsov, Zh. Eksp. Teor. Fiz. **54**, 826 (1968).
[40] D. Emin, and T. Holstein, Ann. Phys. **53**, 439 (1969).
[41] H. Frölich, *Theory of Dielectric* (Clarendon, Oxford, 1958), p. 70.
[42] R. Gerhardt, J. Phys. Chem. Solids **55**, 1491 (1994).
[43] R. Gehlig and E. Salje, Philos. Mag. B **47**, 229 (1983).
[44] E. Iguchi, N. Kubota, T. Nakamori, N. Yamamoto, and K. J. Lee, Phys. Rev. B **43**, 8646 (1991).
[45] E. Iguchi and K. Akashi, J. Phys. Soc. Jpn. **61**, 3385 (1992).